Earth and Planetary Science Letters 433 (2016) 370–379

Contents lists available at ScienceDirect

Earth and Planetary Science Letters

www.elsevier.com/locate/epsl

# Development of a regional glycerol dialkyl glycerol tetraether (GDGT)–temperature calibration for Antarctic and sub-Antarctic lakes

Louise C. Foster [a,b,*], Emma J. Pearson [b], Steve Juggins [b], Dominic A. Hodgson [a], Krystyna M. Saunders [c], Elie Verleyen [d], Stephen J. Roberts [a]

[a] British Antarctic Survey, Natural Environment Research Council, High Cross, Madingley Road, Cambridge, CB3 0ET, UK
[b] School of Geography, Politics and Sociology, Newcastle University, Newcastle-upon-Tyne, NE1 7RU, UK
[c] Institute of Geography and the Oeschger Centre for Climate Change Research, University of Bern, 3012, Bern, Switzerland
[d] Ghent University, Protistology and Aquatic Ecology, Krijgslaan 281 S8, 9000 Gent, Belgium

ARTICLE INFO

*Article history:*
Received 2 September 2015
Received in revised form 7 November 2015
Accepted 12 November 2015
Available online 29 November 2015
Editor: D. Vance

*Keywords:*
palaeoclimate
temperature reconstruction
GDGTs
Southern Hemisphere
palaeolimnology
Antarctic

ABSTRACT

A regional network of quantitative reconstructions of past climate variability is required to test climate models. In recent studies, temperature calibration models based on the relative abundances of sedimentary glycerol dialkyl glycerol tetraethers (GDGTs) have enabled past temperature reconstructions in both marine and terrestrial environments. Nevertheless, to date these methods have not been widely applied in high latitude environments due to poor performance of the GDGT–temperature calibrations at lower temperatures. To address this we studied 32 lakes from Antarctica, the sub-Antarctic Islands and Southern Chile to: 1) quantify their GDGT composition and investigate the environmental controls on GDGT composition; and 2) develop a GDGT–temperature calibration model for inferring past temperatures from Antarctic and sub-Antarctic lakes. GDGTs were found in all 32 lakes studied and in 31 lakes branched GDGTs (brGDGTs) were the dominant compounds. Statistical analyses of brGDGT composition in relation to temperature, pH, conductivity and water depth showed that the composition of brGDGTs is strongly correlated with mean summer air temperature (MSAT). This enabled the development of the first regional brGDGT–temperature calibration for use in Antarctic and sub-Antarctic lakes using four brGDGT compounds (GDGT-Ib, GDGT-II, GDGT-III and GDGT-IIIb). A key discovery was that GDGT-IIIb is of particular importance in cold lacustrine environments. The addition of this compound significantly improved the model's performance from $r^2 = 0.67$, RMSEP-LOO (leave-one-out) = 2.23 °C, RMSEP-H (*h*-block) = 2.37 °C when applying the re-calibrated global GDGT–temperature calibration to our Antarctic dataset to $r^2 = 0.83$, RMSEP-LOO = 1.68 °C, RMSEP-H = 1.65 °C for our new Antarctic calibration. This shows that Antarctic and sub-Antarctic, and possibly other high latitude, palaeotemperature reconstructions should be based on a regional GDGT–temperature calibration where specific compounds can be identified and included to improve model performance. Finally, downcore temperature reconstructions using the new Antarctic brGDGT–temperature calibration were tested in sub-Antarctic Fan Lake from South Georgia providing a proof of concept for the new calibration model in the Southern Hemisphere.



## 1. Introduction

Previous studies of past climates in high-latitude regions have used a range of biological proxies including changes in accumulation rates and species composition of pollen, diatoms, pigments and chironomids to give indirect qualitative or quantitative inferences about past environmental changes (e.g., Anderson et al., 2001; Verleyen et al., 2003; Hodgson et al., 2005; Rolland et al., 2009; Watcham et al., 2011; Strother et al., 2015). Many of these proxies respond to a range of environmental controls, including pH, salinity or atmospheric circulation, all of which can influence their ability to accurately quantify past changes in temperature (Shanahan et al., 2013). Moreover, in the harsh Antarctic environment, palaeoclimate techniques are restricted due to the biological proxies being limited or absent, so there is a real need for a robust method to quantify temperature. This is particularly important in Antarctic lakes where quantitative temperature reconstructions using biogeochemical proxies in lake sediment cores will enable a

* Corresponding author at: British Antarctic Survey, Natural Environment Research Council, High Cross, Madingley Road, Cambridge, CB3 0ET, UK.
*E-mail address:* l.c.foster@gmx.co.uk (L.C. Foster).

http://dx.doi.org/10.1016/j.epsl.2015.11.018

substantial improvement in our understanding of past atmospheric temperature at low altitudes without the complicating factors of changing ocean currents (which limit the application of marine-based palaeothermometry through redistributing heat e.g., Kim et al., 2012) and high altitude temperature effects (which apply to most ice core reconstructions e.g., Mulvaney et al., 2012).

One such approach is the application of glycerol dialkyl glycerol tetraethers (GDGTs). Several studies have used changes in the relative abundance of GDGTs in ocean sediments (e.g., Schouten et al., 2002; Kim et al., 2010; Tierney and Tingley, 2014), soils (e.g., Weijers et al., 2007a; Peterse et al., 2012) and lake sediments (e.g., Powers et al., 2005; Tierney et al., 2010; Pearson et al., 2011; Loomis et al., 2012) for quantitatively reconstructing past temperature. GDGTs are cell membrane lipids found in archaea and bacteria and their structure strongly depends on growth temperature (Schouten et al., 2002; Weijers et al., 2006). More specifically, the number of cyclopentane rings in the GDGT structure is a key factor in the adaptation to temperature change (Gliozzi et al., 1983; Uda et al., 2001; Schouten et al., 2002). To date GDGTs have only been studied in seven Antarctic and sub-Antarctic lakes as part of the Pearson et al. (2011) global calibration model. In these few sites the GDGT–temperature relationship does not appear to be as strong as the global relationship, suggesting a need to expand upon and further investigate the environmental controls on GDGT composition in Antarctic lakes.

### 1.1. GDGTs in lacustrine environments

Powers et al. (2004, 2005) first investigated the use of GDGTs in lacustrine environments, developing a lacustrine variation of the marine $TEX_{86}$ index, and demonstrated its potential as a temperature proxy in large lakes. However, its dependence on isoprenoid GDGTs (isoGDGTs), which are frequently in low abundance in lakes, means $TEX_{86}$ is often not applicable. The Branched Isoprenoid Tetraether (BIT) index is the ratio of branched GDGTs (brGDGTs) to isoGDGTs which can be used to identify lakes with a high proportion of brGDGTs and thus where the $TEX_{86}$ index will be unreliable (e.g., BIT > 0.5; Hopmans et al., 2004; Weijers et al., 2006; Blaga et al., 2009). This interpretation must be approached with caution as Weijers et al. (2007a), Tierney et al. (2010) and Pearson et al. (2011) all found that the BIT value was predominantly related to low concentrations of Crenarchaeol, an isoGDGT, rather than a high abundance of brGDGTs.

Alternatively, the soil MBT/CBT index, developed by Weijers et al. (2007a) uses brGDGTs which often dominate the GDGT composition in lacustrine environments. Although several studies have applied this MBT/CBT soil index in lakes (e.g., Sinninghe Damsté et al., 2009; Tierney et al., 2010; Sun et al., 2011; Loomis et al., 2012; Naeher et al., 2014), it can underestimate measured temperatures by up to 15 °C.

The limitations of $TEX_{86}$ and MBT/CBT indices has led to the development of GDGT–temperature calibrations specific to lacustrine environments, including a global brGDGT–temperature regression model by Pearson et al. (2011) and regional models for East Africa by Tierney et al. (2010) and Loomis et al. (2012). Pearson et al. (2011) used the fractional abundances of brGDGTs to develop a global calibration using 85 lakes from the Scandinavian Arctic to Antarctica and applied best subsets regression to select a subset of brGDGT compounds with optimal predictive properties for mean summer air temperature (MSAT) (Eq. (1)).

$$\mathrm{MSAT} = 20.9 + (98.1 \times \text{GDGT-Ib}) - (12.0 \times \text{GDGT-II}) - (20.5 \times \text{GDGT-III}) \quad (1)$$

This global calibration has a high accuracy and precision ($r^2$ = 0.88, RMSE = 2.0 °C, RMSEP = 2.1 °C) and is not significantly influenced by pH, conductivity or water depth. Naeher et al. (2014) applied the model to Lake Rotsee, Switzerland and found good correlation between reconstructed and measured temperatures.

Loomis et al. (2012) developed a regional East African brGDGT–temperature calibration for mean annual air temperature (MAAT) (Eq. (2)) adding 70 lakes to the 41 studied by Tierney et al. (2010), and adding one additional brGDGT compound (GDGT-IIc) to those used by Pearson et al. (2011).

$$\mathrm{MAAT} = 22.77 - (35.58 \times \text{GDGT-III}) - (12.88 \times \text{GDGT-II}) - (418.53 \times \text{GDGT-IIc}) + (86.43 \times \text{GDGT-Ib}) \quad (2)$$

Although GDGT-IIc does not have a significant relationship with temperature in the global dataset of Pearson et al. (2011), it does improve model performance in the East African regional model. Loomis et al. (2012) concluded that regional calibrations had better predictive ability compared with global calibrations. Regional calibrations can only be achieved where temperature gradients are sufficiently large. In the East Africa dataset this is achieved by sampling lakes along an altitudinal gradient.

Sinninghe Damsté et al. (2012) applied both the Tierney et al. (2010) and the Pearson et al. (2011) brGDGT–temperature calibrations in Lake Challa, equatorial Africa, finding that the temperature difference between the Last Glacial Maximum and the Holocene for both calibrations was consistent with previous temperature reconstructions by Powers et al. (2005), Weijers et al. (2007b) and Tierney et al. (2008). More recently, Woltering et al. (2014) applied ten different GDGT–temperature calibrations, including both soil and lake calibrations, to a core from Lake McKenzie, Australia. They showed that although all calibrations indicated significantly lower temperatures during the last glacial period, the choice of calibration affected both the trend and absolute values of the reconstructed temperatures, highlighting the need for careful choice of calibration model (Woltering et al., 2014, Fig. 4).

Equation (1) provides the best fit calibration with minimum prediction error across a wide range of temperatures for Pearson et al.'s (2011) global dataset, but the model included only six sites with MSAT below 5 °C and none below 1.5 °C. As a consequence, it performs relatively poorly at low temperatures and overestimated MSAT in this part of the gradient (Pearson et al., 2011, Fig. 7b).

To address this limitation we studied 32 lakes from Antarctica, the sub-Antarctic Islands and Southern Chile, adding 26 new lakes to the high latitude Southern Hemisphere lakes studied by Pearson et al. (2011). Combining the two datasets we had a total of 37 samples including five replicate samples from sites included in Pearson et al. (2011) and re-sampled as part of this study. The aims of this paper are to: 1) quantify the GDGT composition of lake surface sediments and investigate the environmental controls on GDGT composition in Antarctic and sub-Antarctic lakes; 2) develop a brGDGT–temperature calibration for inferring past temperatures from Antarctic and sub-Antarctic lakes; and 3) test the calibration on a lake-sediment core from the sub-Antarctic.

## 2. Materials and methods

### 2.1. Study locations

Surface sediments (top 0–2 cm) from 32 lakes from Antarctica, the sub-Antarctic Islands and Southern Chile (Fig. 1) were collected using a UWITEC surface gravity corer during several field campaigns in the Southern Hemisphere spring–summer season. Sites spanned a range of MAAT from −11.8 to 6.1 °C and MSAT (December to February) from −2.2 to 10.3 °C. The sites also covered a range of pH (4.5 to 9.8), conductivity (0.01 to 7.38 mS cm$^{-1}$) and water depths (0.5 to 55 m). A summary of the temperature and limnological data for lakes in each region is listed in Table 1 and outlined for each individual lake in Supplementary Table S1.

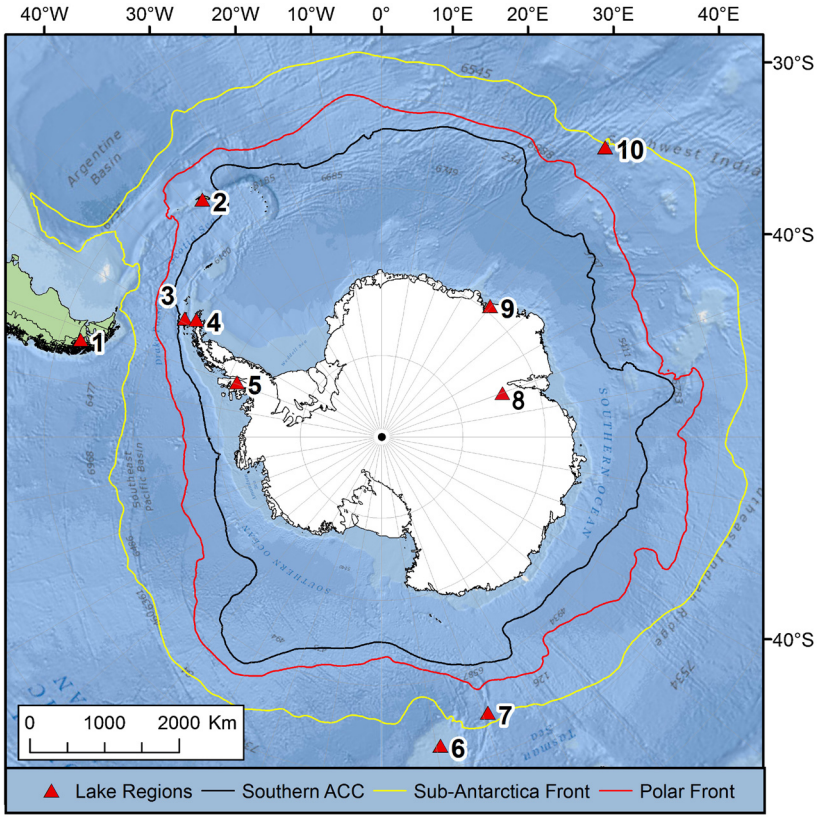


**Fig. 1.** Map of the locations of the lake surface sediments: 1) Southern Chile, 2) Annenkov Island, South Georgia, 3) South Shetland Islands, 4) Trinity Peninsula, 5) Alexander Island, 6) Campbell Island, 7) Macquarie Island, 8) Larsemann Hills, 9) Syowa Oasis and 10) Marion Island. Background image is a compilation of the General Bathymetric Chart of the Oceans GEBCO_08 Grid, IHO-IOC GEBCO Gazetteer of Undersea Feature Names, National Oceanic and Atmospheric Administration (NOAA), and National Geographic, DeLorme, NAVTEQ, Geonames.org, and Esri, and various other contributors, downloaded from the British Oceanographic Data Centre (BODC) https://www.bodc.ac.uk/data/online_delivery/gebco.

The 4000 cal yr BP to present section of a previously published c. 7700-year-old sediment core from sub-Antarctic Fan Lake (54°29′0″S, 37°5′0″W), on Annenkov Island, South Georgia, (Fig. 1) was used to test the Antarctic and sub-Antarctic brGDGT–temperature calibration. Fan Lake is approximately 430 m long, 200 m wide and 18 m deep at its deepest point in the centre of the lake. During sampling, in December 2005, its stratification regime was cold polymictic with a near-surface water temperature of 4.6 °C and a basal water temperature of 4.4 °C (Pearson et al., 2011; Strother et al., 2015). No year-round temperature data are available for Fan Lake, but comparison with lakes at similar latitudes in the Southern Hemisphere, suggests the surface water temperature would decline during the Austral winter when the lake is ice-covered (Strother et al., 2015). Details of the sedimentology of a 5.8 m long core and its Bayesian age–depth model, which is based on $^{210}$Pb dating of the top 11 cm of the core and 32 radiocarbon dates, can be found in Strother et al. (2015).

### 2.2. GDGT extraction and analysis

GDGTs were extracted from 0.1 to 2.9 g of freeze dried and homogenised sediment. The samples were microwave extracted using DCM:methanol (3:1, v:v). The total extracts were saponified and GDGTs isolated using hexane extractions following Pearson et al. (2011). The GDGT extracts were filtered through a 0.2 µm Whatman PTFE filter prior to analysis using an Acquity Xevo TQ-S (triple quadrupole with step wave; Waters Ltd.) LC-MS set up with an atmospheric pressure chemical ionisation (APCI) source (Ion saber II) operated in positive ion mode. Analytical separation was achieved using a Grace Prevail Cyano HPLC column (3 µm, 150 × 2.1 mm i.d.) fitted with an in line filter (Waters Acquity UPLC in-line filter, 0.2 µm) at 40 °C using a binary solvent gradient where eluent A was hexane and eluent B was propanol. The flow rate of the mobile phase was 0.2 ml per minute with a gradient profile of 99% A 1% B (0–50 min); 98.2% A 1.8% B (50–55 min); 90% A 10% B (55–65 min) and finally 99% A 1% B (66–80 min). The LC-MS settings were: source offset 50 V, capillary 1.5 KV, desolvation temperature 200 °C, cone voltage 30 V, desolvation gas ($N_2$). All sediment analysis was done at Newcastle University using HPLC grade solvents purchased from Fisher (Loughborough, UK).

Detection was achieved using selected ion monitoring (SIM) of targeted $[M + H]^+$ ions (dwell time 50 ms). The target ions were m/z 1302, 1300, 1298, 1296 and 1292 for the isoGDGTs and 1050, 1048, 1046, 1036, 1034, 1032, 1022, 1020 and 1018 for the brGDGTs. Peak identification and integration was carried out using MassLynx software (version 4.1).

### 2.3. Environmental data

Environmental data were collected from a range of sources including unpublished field reports from the British Antarctic Survey and other collaborators, research stations and previously published research (see Supplementary Table S1 for data). Air temperatures were used as a surrogate for lake water temperature based on their strong relationship with the latter (Edinger et al., 1968; Webb and Nobilis, 1997; Livingstone and Dokulil, 2001). Following Pearson et al. (2011), we used MSAT rather than MAAT for two reasons. First, Antarctic lakes are rarely monitored all year round, and lake water temperature data are largely restricted to the austral summer and/or when lakes were cored or otherwise investigated. Second, many lakes remain ice-covered for much of the year and mean annual temperatures are not a bio-

**Table 1**
Lake temperature and environmental characteristics summarised by region.

| Region | Number of lakes | Latitude | | Longitude | | Altitude (m) | | Water depth (m) | | MAAT (°C) | | MSAT (°C) | | Conductivity (mS/cm) | | pH | |
|---|---|---|---|---|---|---|---|---|---|---|---|---|---|---|---|---|---|
| | | Min | Max | Min | Max | Min | Max | Min | Max | Min | Max | Min | Max | Min | Max | Min | Max |
| Alexander Island | 2 | S 70.85 | S 71.78 | W 68.25 | W 68.33 | 98.0 | 126.0 | 5.6 | 55.0 | −5.1 | −4.9 | 0.1 | 0.3 | 0.058 | 0.158 | 6.67 | 7.97 |
| Campbell Island | 4 | S 52.51 | S 52.59 | E 169.15 | E 169.19 | 268.0 | 379.0 | 0.9 | 1.2 | 3.8 | 4.8 | 6.0 | 7.0 | 0.117 | 0.287 | 4.46 | 5.07 |
| Fildes Peninsula | 5 | S 62.20 | S 62.23 | W 58.96 | W 58.98 | 14.5 | 34.5 | 5.3 | 7.0 | −2.5 | −2.4 | 1.0 | 1.1 | 0.013 | 0.177 | 7.53 | 8.07 |
| Larsemann Hills | 4 | S 69.38 | S 69.41 | E 76.05 | E 76.40 | 5.0 | 65.0 | 3.8 | 38.0 | −11.8 | −11.2 | −2.2 | −1.6 | 0.261 | 7.380 | 6.30 | 7.10 |
| Marguerite Bay | 1 | S 67.60 | S 67.60 | W 67.20 | W 67.20 | 19.4 | 19.4 | 6.1 | 6.1 | −4.5 | −4.5 | 0.7 | 0.7 | 0.131 | 0.131 | 6.54 | 6.54 |
| Marion Island | 3 | S 46.86 | S 46.86 | E 37.85 | E 37.85 | 71.0 | 98.0 | 0.9 | 1.0 | 4.6 | 4.8 | 6.7 | 6.8 | 0.061 | 0.069 | 6.46 | 7.85 |
| Potter Peninsula | 2 | S 62.24 | S 62.25 | E 58.66 | E 58.67 | 21.0 | 35.0 | 2.2 | 5.6 | −1.9 | −1.8 | 1.0 | 1.1 | 0.050 | 0.050 | 6.17 | 6.40 |
| South Georgia | 1 | S 54.50 | S 54.50 | W 37.05 | W 37.05 | 94.0 | 94.0 | 18.0 | 18.0 | 1.6 | 1.6 | 4.4 | 4.4 | 0.038 | 0.038 | 8.07 | 8.07 |
| Southern Chile | 2 | S 51.30 | S 53.60 | W 70.95 | W 72.67 | 3.0 | 50.0 | 4.4 | 17.0 | 5.8 | 6.1 | 10.0 | 10.3 | 0.246 | 0.301 | 8.64 | 8.81 |
| Syowa Oasis | 4 | S 69.03 | S 69.47 | E 39.51 | E 39.61 | −10.0 | 5.0 | 2.2 | 6.0 | −10.7 | −10.6 | −2.0 | −1.9 | 0.273 | 0.668 | 7.64 | 8.95 |
| Trinity Peninsula | 4 | S 63.55 | S 63.61 | W 57.34 | W 57.41 | 2.5 | 134 | 0.5 | 24.0 | −5.9 | −5.1 | −0.4 | −0.4 | 0.035 | 0.470 | 7.37 | 9.80 |

logically relevant parameter in regions with large seasonal temperature fluctuations or where long periods of ice cover exist. Shanahan et al. (2013) confirmed a seasonal pattern in brGDGT production in Arctic lakes where production increased during the summer when temperatures were warmest and lakes were ice free. For each lake air temperature data were taken from the nearest research station and MSAT calculated by taking an average of the December, January and February mean air temperatures for a ten year period. Finally, temperatures were lapse rate corrected using regional specific lapse rates from previous research in the region (e.g., Braun et al., 2004; Magand et al., 2004).

### 2.4. Statistical analysis

Previous lacustrine studies have shown a strong correlation between brGDGTs and temperature (e.g., Tierney et al., 2010; Pearson et al., 2011; Sun et al., 2011; Loomis et al., 2012; Shanahan et al., 2013), therefore we focused on the brGDGT compounds only, and individual brGDGTs were normalised to a percentage of the total brGDGTs prior to all numerical analysis.

The relationship between brGDGT composition and environmental conditions was explored using redundancy analysis (RDA) (see Pearson et al., 2011). RDA is a form of constrained principal components analysis in which variations in GDGT composition are directly related to lake physical–chemical characteristics. The relative strength and statistical independence of each environmental variable was assessed using a series of RDAs and partial RDAs to partition the variation in brGDGT composition into the (a) total, and (b) unique, or independent, effect, of each variable (Borcard et al., 1992). The statistical significance of each component of variation was assessed using a Monte-Carlo permutation test.

To develop the brGDGT–temperature calibration for our Antarctic dataset we used best subsets regression to select an optimal set of brGDGT compounds that yielded minimum prediction errors. Errors estimated from the original regression model suffer from resubstitution bias, and will generally underestimate true prediction error when the model is applied to new data outside of the calibration set. A method of cross-validation, such as leave-one-out (LOO), is therefore usually employed to provide a more accurate estimate of model performance (e.g., Pearson et al., 2011). However, LOO fails to account for the effects of spatial autocorrelation and pseudoreplication that may exist in spatially structured calibration data, and consequently yields an over-optimistic estimate of prediction error (Telford and Birks, 2005). We therefore use Mantel correlograms (Borcard et al., 2011) and multivariate variograms (Dray et al., 2006) to identify the extent of spatial dependency in the brGDGT and associated temperature data, and then cross-validate our model using a so-called *h*-block procedure. This involves obtaining a prediction for a calibration sample where that sample, and its neighbours with a distance of '*h*', are omitted from the calibration set (Burman et al., 1994). To facilitate comparison with earlier work we summarise model performance using four measures: the squared correlation between observed and predicted MSAT for the calibration set ($r^2$); the root mean squared error for the calibration set (RMSE); the RMSE estimated by LOO; and *h*-block cross-validation (RMSEP-LOO and RMSEP-H, respectively).

Lake depth and lake water conductivity had right skewed distributions and were either square-root (depth) or $\log_{10}$, (conductivity) transformed prior to all numerical analyses. R software for statistical computing and graphics (R Core Team, 2014) with the packages vegan (Oksanen et al., 2014), leaps (Lumley, 2009), and rioja (Juggins, 2014) was used for all numerical analyses.

### 2.5. Fan Lake downcore analysis

Total organic carbon (TOC) and total nitrogen (TN; not used in this study) analysis was undertaken as part of an investigation into the stable carbon isotope composition of the Fan Lake c. 8000 cal yr BP to present core sequence. Here, we present new TOC data for the post 4000 cal yr BP section of the core. Sediment samples were freeze-dried, and homogenised. Carbonate was removed using 5% HCl for 24 hours and samples were washed and dried prior to analysis. TOC and TN were determined simultaneously with bulk organic carbon isotopic ratios ($\delta^{13}C_{org}$) by combustion on a Carlo Erba 1500 on-line to a VG Triple Trap and Optima dual-inlet mass spectrometer at NIGL (NERC Isotope Geosciences Laboratory). $\delta^{13}C_{org}$ values were calculated to the VPDB scale using a within-run laboratory standard calibrated against NBS-19 and NBS-22. For further comparison, TOC and TN concentrations (%) were also determined on selected replicate samples by combustion on a Flash 2000 Organic Elemental Analyser at the University of Ghent (Thermo-Scientific/Interscience), with reproducibility and reliability of the analyses tested using standards of sulphanilamide. The replicate analyses of randomly selected samples from the whole Fan Lake core gave a precision of ±0.1 (per mil) for $\delta^{13}C_{org}$ and <10% for TOC ($n = 12$; mean ± std. err. = 3.17 ± 0.16; 5.0% std. error). Palynological samples were processed and analysed in the laboratories at Northumbria University, Newcastle, and Durham University following standard procedures described in Strother et al. (2015).

The sedimentary flux of TOC and catchment-derived pollen proxy data were calculated by multiplying the sediment dry bulk density (g cm$^{-3}$) by the sedimentation rate (cm yr$^{-1}$) and the concentration for the relevant dataset following standard procedures in Street-Perrot et al. (2007). Sedimentation rates were calculated from the Fan Lake age–depth model in Strother et al. (2015). Dry bulk density was calculated from contiguous 1 cm interval, 1 cm$^3$ subsamples and standard loss-on-ignition (LOI) procedures: 12 hrs drying at 110 °C followed by 2 hrs at 550 °C, and 4 hrs at 950 °C to determine dry mass (g), organic and carbonate content based on % weight loss on ignition (LOI) after combustion (following Dean, 1974).

## 3. Results

### 3.1. Environmental controls on brGDGT composition

GDGTs were found in all 32 lakes although only 11 lakes had a full suite of isoGDGTs (Fig. 2). BrGDGTs were the dominant compounds in 31 lakes. In Moutonnée Lake isoGDGTs were anomalously abundant, likely due to its hydraulic connection to the seawater in George VI Sound (Smith et al., 2007; Roberts et al., 2008, 2009). This site was therefore excluded from further analysis leaving 36 samples, including replicates, from 31 lakes. The BIT index values of the 31 remaining lakes ranged from 0.71 to 1.0 with the majority (88.9%) having a BIT >0.95 (Fig. 2). The BIT value showed a strong correlation with Crenarchaeol abundance ($r = -0.999$, $p < 0.001$) and a weak but significant correlation with brGDGT abundance ($r = 0.40$, $p = 0.018$).

RDAs and associated permutation tests using individual environmental variables as explanatory variables showed that only MSAT, pH and lake depth explained significant portions of variation in brGDGT composition. Other environmental variables were therefore excluded from further analysis. The first and second components of the RDA (Fig. 3a and 3b) summarise the relationship between the nine branched GDGT compounds with the three significant environmental variables and accounts for 33.8% and 5.1% of the variance in brGDGT composition, respectively. Component 1 reflects a gradient from higher pH and depth and lower temperatures on the left, to lakes with higher pH, greater depth and higher temperatures to the right of the ordination diagram (Fig. 3a). GDGT-I, GDGT-II and GDGT-III all have weak but significant correlations with depth ($r = -0.37$, $-0.33$ and 0.40 respectively, $p \leq 0.05$). Significant relationships were also found between GDGT-I, GDGT-Ib, GDGT-Ic and GDGT-III and pH ($r = -0.40$, $-0.36$, $-0.55$, 0.37, $p \leq 0.05$, respectively).

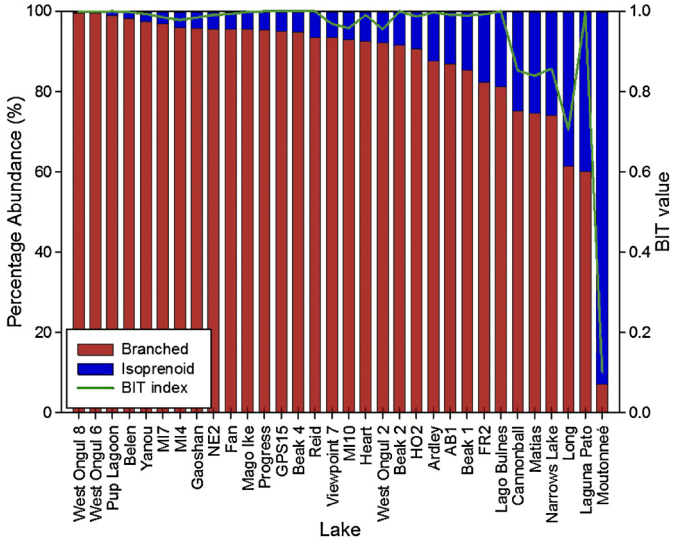


**Fig. 2.** Bar chart showing relative distributions of branched and isoprenoid GDGTs, and BIT index, in the lake surface sediments.

Temperature had a strong and significant positive correlation with GDGT-I, GDGT-Ib and GDGT-IIIb ($r = 0.63$, 0.66 and 0.76, respectively) and a weaker but still significant positive correlation with GDGT-Ic ($r = 0.45$) (Fig. 3b). Conversely temperature had a negative correlation with GDGT-III ($r = -0.57$; all $p < 0.005$) (Fig. 3b). Component 2 is negatively correlated to pH and depth, and reflects a small amount of residual variation (5.1%) due to these variables independent of MSAT.

Variance partitioning (Fig. 3c) indicated that MSAT accounts for the largest fraction of variance in brGDGT composition (29.5%) and that the effect of MSAT was largely independent of other variables, with only 7.8% shared with pH and water depth. pH and depth account for 11.4% and 10.1% of the variance respectively, but only have a small independent effect on brGDGT composition (2.6% and 1.2%, respectively; Fig. 3c).

### 3.2. Development of a new brGDGT–temperature calibration for Antarctic and sub-Antarctic lakes

To address the limitations of existing GDGT–temperature calibrations in cold environments we developed a regional calibration for Antarctic and sub-Antarctic lakes. Initially, this was based on multiple regression using the set of compounds included in the Pearson et al. (2011) global calibration, but re-calibrated using our expanded surface sample Antarctic GDGT dataset (Fig. 4a). Results of the Mantel correlograms and multivariate variograms (not shown) both indicate spatial dependency in the GDGT data at distances up to 500 km. We therefore use this distance as the cut-off value for $h$-block cross-validation.

$$\mathrm{MSAT} = 32.5 + (85.4 \times \mathrm{GDGT\text{-}Ib}) - (43.1 \times \mathrm{GDGT\text{-}II}) - (32.1 \times \mathrm{GDGT\text{-}III}) \quad (3)$$

$$\left(r^2 = 0.67, \mathrm{RMSE} = 2.00\,^{\circ}\mathrm{C}, \mathrm{RMSEP\text{-}LOO} = 2.23\,^{\circ}\mathrm{C}, \mathrm{RMSEP\text{-}H} = 2.37\,^{\circ}\mathrm{C}, n = 36\right)$$

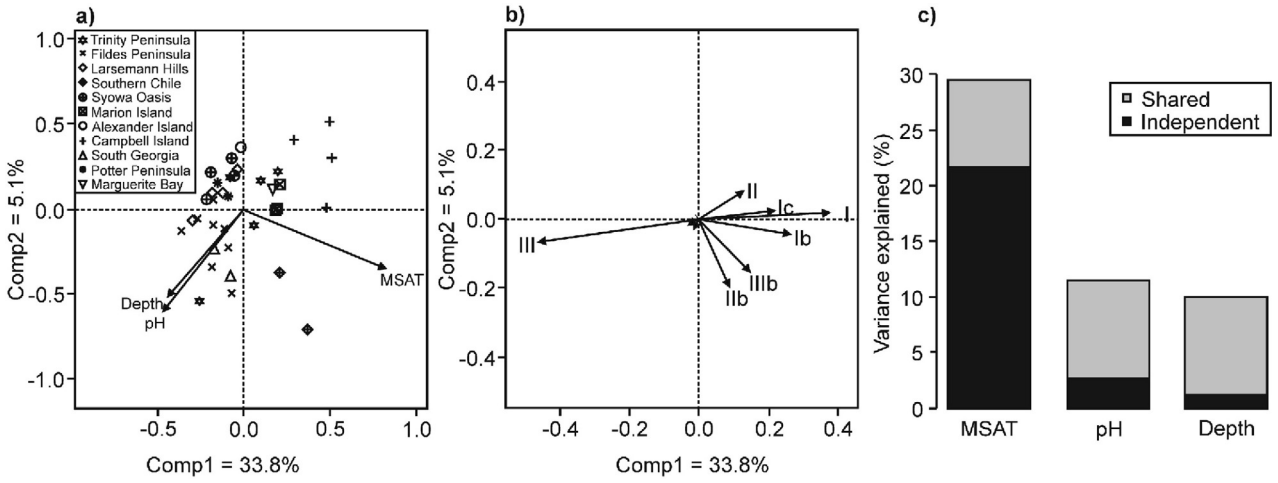


**Fig. 3.** Plots showing the results of the redundancy analysis (RDA) and variance partitioning: a) ordination plot showing the relationships between sites and environmental variables and b) their relationship with the branched GDGT composition. c) Bar chart showing the percentage variance in GDGT composition explained by MSAT, pH, and depth.

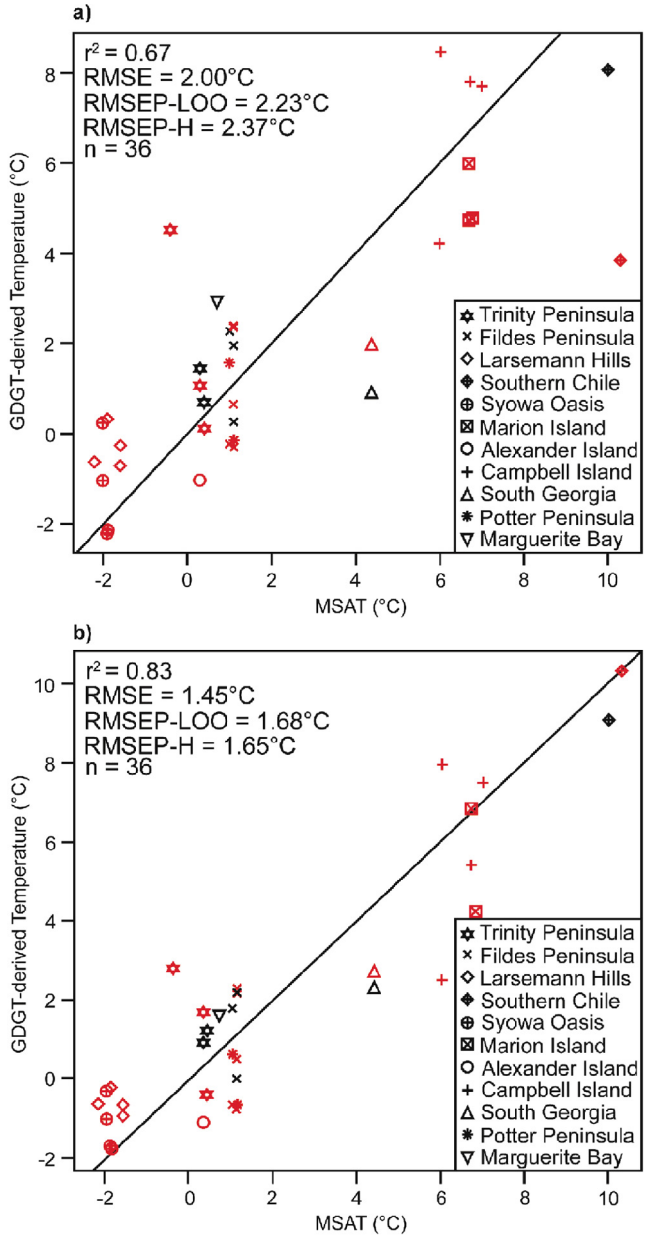


**Fig. 4.** Relationships between measured temperature and GDGT-calibrated temperature for regression models based on (a) the compounds used in Pearson et al. (2011) (Eq. (3)) and (b) new best subsets regression model for Antarctica (Eq. (4)). The black points are data taken from Pearson et al. (2011) and the red points from this study. Symbols indicate the location of the surface sediments. (For interpretation of the references to colour in this figure legend, the reader is referred to the web version of this article.)

We then developed a regression model using best subsets regression (Fig. 4b) to select a set of compounds with optimal predictive properties. This model included GDGT-IIIb as an additional predictor:

$$\mathrm{MSAT} = 18.7 + (80.3 \times \mathrm{GDGT\text{-}Ib}) - (25.3 \times \mathrm{GDGT\text{-}II}) - (19.4 \times \mathrm{GDGT\text{-}III}) + (369.9 \times \mathrm{GDGT\text{-}IIIb}) \quad (4)$$

$$\left(r^2 = 0.83, \mathrm{RMSE} = 1.45\,^{\circ}\mathrm{C}, \mathrm{RMSEP\text{-}LOO} = 1.68\,^{\circ}\mathrm{C}, \mathrm{RMSEP\text{-}H} = 1.65\,^{\circ}\mathrm{C}, n = 36\right)$$

Compared to the Antarctic dataset brGDGT–temperature calibration using the same compounds as Pearson et al. (2011) (Eq. (3); Fig. 4a), the new calibration (Eq. (4); Fig. 4b) has an increased $r^2$ (0.83) and substantially lower RMSE under both LOO (1.68 °C) and $h$-block (1.65 °C) cross-validation (Table 2). Additionally, the replicate samples from the same lake, as analysed as part of this study and previously by Pearson et al. (2011), plot close to one another when applying the Antarctic and sub-Antarctic calibration (Eq. (4); Fig. 4b) showing good reproducibility in the method. Finally, the residuals of the Antarctic and sub-Antarctic GDGT–temperature calibration were not significantly correlated with pH ($r = 0.18$, $p = 0.29$), depth ($r = 0.14$, $p = 0.42$) or conductivity ($r = 0.28$, $p = 0.10$).

### 3.3. Application of the brGDGT–temperature calibration

In the 4000 year Fan Lake record the reconstructed temperatures were between 2.2 and 13.7 °C (Antarctic and sub-Antarctic calibration) and 5.7 and 8.7 °C (global calibration). The warmest temperatures were reconstructed at c. 3400 cal yr BP when applying the Antarctic and sub-Antarctic calibration and for the global calibration at c. 3700 cal yr BP (Fig. 5). Reconstructed core top temperatures were 2.2 and 6.6 °C respectively, compared to a measured MSAT of 4.4 °C.

**Table 2**
Equation and model statistics including $r^2$, $p$, RMSE and RMSEP for the application of: the global brGDGT–temperature calibration (Pearson et al., 2011), an Antarctic brGDGT–temperature calibration based on the same three compounds used in the global calibration and our new Antarctic brGDGT–temperature calibration which also includes GDGT-IIIb.

| Calibration equation | | $r^2$ | $p$ value | RMSE (°C) | RMSEP-LOO (°C) | RMSEP-H (°C) |
|---|---|---|---|---|---|---|
| Pearson et al. (2011) | MSAT = 20.9 + (98.1 × GDGT-Ib) − (12.0 × GDGT-II) − (20.5 × GDGT-III) | 0.54 | <0.001 | 2.32 | N/A | N/A |
| Antarctic calibration based on Pearson et al. (2011) compounds | MSAT = 32.5 + (85.4 × GDGT-Ib) − (43.1 × GDGT-II) − (32.1 × GDGT-III) | 0.67 | <0.001 | 2.00 | 2.23 | 2.37 |
| New Antarctic calibration | MSAT = 18.7 + (80.3 × GDGT-Ib) − (25.3 × GDGT-II) − (19.4 × GDGT-III) + (369.9 × GDGT-IIIb) | 0.83 | <0.001 | 1.45 | 1.68 | 1.65 |

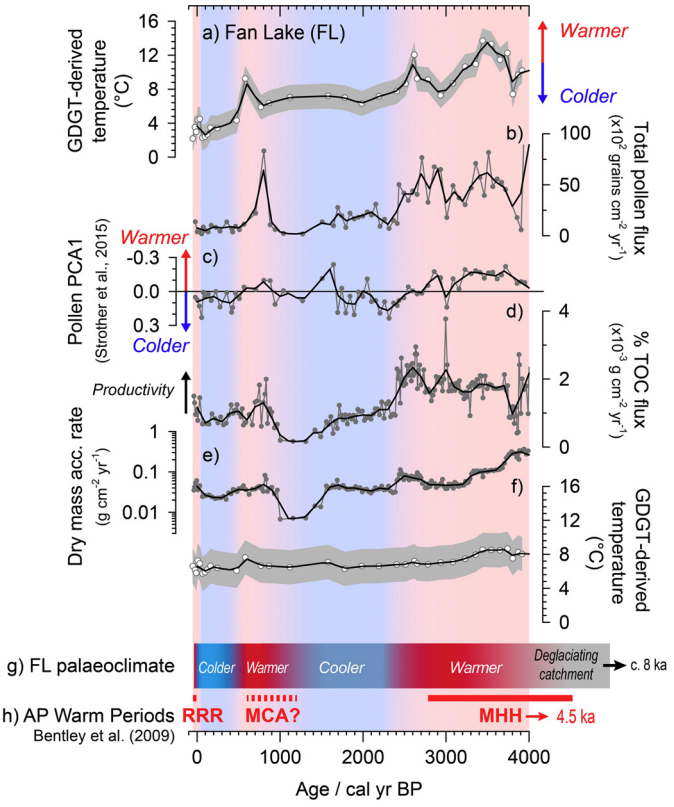


**Fig. 5.** (a) GDGT-derived temperature for the last 4000 years of the Fan Lake (FL), Annenkov Island (near South Georgia) sediment record based on the new Antarctic and sub-Antarctic GDGT–temperature calibration model (this study) compared with previously published productivity proxy data from Fan Lake: (b) total pollen concentration corrected for changes in dry sediment mass accumulation rate (MAR) (as shown in (e)) and referred to as total pollen flux) (data in Strother et al., 2015 recalculated for this study); (c) pollen species Principal Component Analysis (PCA) axis 1 summary data interpreted by Strother et al. (2015) as representing warmer–colder temperature shifts; (d) percentage Total Organic Carbon (TOC) flux (this study); (e) dry MAR changes (this study); (f) GDGT-derived temperature from Fan Lake, reconstructed using the Pearson et al. (2011) global calibration dataset (this study); (g) an interpretation of the Fan Lake palaeoclimate from the combined records; (h) the composite timing of the key mid–late Holocene warm periods identified in most Antarctic Peninsula (AP) palaeo-records (Bentley et al., 2009): MHH = Mid Holocene Hypsithermal (4500–2800 cal yr BP), MCA = Medieval Climate Anomaly (1200–600 cal yr BP), RRR = Recent Rapid Regional warming (post 1950 AD).

## 4. Discussion

### 4.1. Environmental controls on GDGT composition in Antarctic and sub-Antarctic lakes

The main finding when analysing the environmental controls on brGDGT composition in Antarctic and sub-Antarctic lakes was that although pH, conductivity, and depth show significant but weak correlations with some brGDGT compounds the relationship between brGDGT composition and temperature is more significant. Moreover, RDA and variance partitioning showed that the main independent environmental control on brGDGT composition in our data set was temperature.

Previous research by Weijers et al. (2007a), Tierney et al. (2010) and Pearson et al. (2011) suggested that BIT values were predominantly related to low Crenarchaeol abundance rather than a high abundance of brGDGTs. The results from our Antarctic and sub-Antarctic lake dataset support these conclusions. Weijers et al. (2007a) also indicated that the cyclisation of GDGTs related to pH as well as temperature, while Tierney et al. (2010) found that GDGT-Ic and GDGT-IIc were correlated with water depth. Nevertheless, Pearson et al. (2011) and Loomis et al. (2012) included cyclic GDGTs in their temperature calibrations as they found no relationship with pH or water depth. Pearson et al. (2011) also assessed the relationship between GDGT-Ib and pH and although they found a significant correlation between GDGT-Ib and pH ($r = 0.29$, $p = 0.008$), the residuals of the brGDGT–temperature calibration were not significantly correlated with pH, suggesting that their model was not confounded by lake-water pH.

In the Antarctic dataset, GDGT-I, GDGT-Ib, and GDGT-Ic all showed a weak negative correlation with pH ($r = -0.33$, $-0.30$, $-0.46$, all $p \leq 0.1$, respectively). GDGT-IIIb showed no significant relationship with pH ($r = 0.16$, $p = 0.355$), conductivity or water depth. Similarly to Pearson et al. (2011), we found that although GDGT-Ib showed a weak correlation with pH, the residuals of the new Antarctic and sub-Antarctic GDGT–temperature calibration model were not significantly correlated to pH (nor to conductivity or water depth). We therefore conclude that our calibration is not confounded by these variables.

Similar relationships between brGDGT compounds and temperature in this research have been identified in previous studies. GDGT-I and GDGT-Ic dominated in warmer environments (Pearson et al., 2011; Loomis et al., 2012; Woltering et al., 2014), whereas in colder environments, such as the Arctic (Shanahan et al., 2013; Peterse et al., 2014), Antarctic and Siberia (Pearson et al., 2011), and the high mountains of the Tibetan Plateau (Günther et al., 2014), GDGT-II and/or GDGT-III dominated over GDGT-I. As expected, GDGT-III or GDGT-II was dominant in every sample in the Antarctic and sub-Antarctic dataset.

### 4.2. Application of the global brGDGT–temperature calibration to the Antarctic dataset

As our dataset is an extension of the original Antarctic, sub-Antarctic and Chilean dataset from Pearson et al. (2011), we applied the global brGDGT–temperature calibration to the Antarctic dataset to evaluate its performance (Table 2; Supplementary Table S2). Previous applications of the global brGDGT–temperature calibration to lakes in Minnesota and Iowa, USA (Schoon et al., 2013), Switzerland (Naeher et al., 2014) and the Canadian

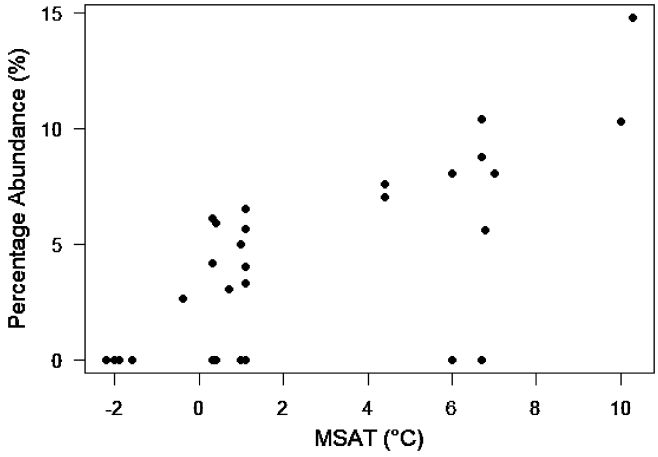


**Fig. 6.** Relationship between GDGT-IIIb abundance and MSAT in the Antarctic and sub-Antarctic lakes dataset.

and Siberian Arctic (Peterse et al., 2014) produced reconstructed temperatures that were comparable with either summer lake or air temperatures. When applying the Pearson et al. (2011) global brGDGT–temperature calibration to our Antarctic dataset the model errors were similar to those of the original global dataset (RMSE = 2.3 °C; Table 2) although the $r^2$ values dropped to 0.54. The Pearson et al. (2011) global model reconstructed temperatures showed a warm bias when compared to MSAT temperatures with an overestimation of temperatures at all sites apart from our warmest site (Lago Bulnes, Chile at 53°S latitude). The average overestimation of the global model in the Antarctic dataset was 6.0 °C with a standard deviation of 2.4 °C.

### 4.3. Assessment of the new Antarctic and sub-Antarctic lakes brGDGT–temperature calibration model

We based our initial Antarctic and sub-Antarctic brGDGT–temperature calibration on the fractional abundances of the same three brGDGTs, GDGT-III, GDGT-II and GDGT-Ib, used in Pearson et al. (2011) (Eq. (3); Fig. 4a). Applying this new calibration to the expanded Antarctic dataset reduced the $r^2$ of the original global calibration from 0.88 to 0.67, but the prediction error of RMSEP-LOO = 2.23 °C, RMSEP-H = 2.37 °C remained comparable to that of the original model (Table 2). There were some notable outliers in the model, for example, the MSAT at Viewpoint on the Trinity Peninsula was −0.4 °C, but the GDGT-derived temperature was 4.5 °C. Conversely, the GDGT-derived temperature at Lago Bulnes of 3.8 °C underestimated the observational data by 6.5 °C (Fig. 4a).

Our new Antarctic and sub-Antarctic brGDGT–temperature calibration (Eq. (4); Fig. 4b) exhibited a higher $r^2$ value of 0.83 and lower overall model errors (RMSE = 1.45 °C, RMSEP-LOO = 1.68 °C and RMSEP-H = 1.73 °C) than the re-calibration of the expanded Antarctic dataset (Eq. (3)). Most importantly, the addition of GDGT-IIIb significantly improved the model and reduced the errors of many of the outliers in the previous calibration (Fig. 4a), most likely because of the strong positive and statistically significant relationship between GDGT-IIIb and temperature ($r = 0.74$, $p < 0.001$; Fig. 6). We therefore conclude that our new calibration equation incorporating GDGT-IIIb is more reliable for reconstructing palaeotemperature from brGDGTs in Antarctic and sub-Antarctic lake sediments.

Significantly, this is the first time that GDGT-IIIb has been used in calibration models despite its presence in lake sediments in previous analyses in East Africa (Loomis et al., 2012) and in the Arctic (Shanahan et al., 2013), with maximum abundances of 2.1% in both regions. Pearson et al. (2011) also found GDGT-IIIb in lakes on a global scale. In our dataset the maximum abundance was similarly low (2.2%). Further investigation showed that below 1 °C the maximum abundance of GDGT-IIIb was 0.4% and below −0.5 °C GDGT-IIIb was below the detection limit. The limited abundance of GDGT-IIIb below c. 1 °C was largely responsible for the increased performance of our regional calibration.

The addition of GDGT-IIIb suggests that, although on a global scale GDGT-Ib, GDGT-II and GDGT-III have a significant relationship with temperature, incorporating additional compounds on a regional scale can significantly improve model performance in particular parts of the temperature gradient. Our new Antarctic and sub-Antarctic brGDGT–temperature calibration may also be applicable in other cold environments, for example the Arctic or high altitudes. To assess the applicability of our calibration to other cold environments further research is needed to determine whether this key relationship between GDGT-IIIb and temperature in Antarctic lakes is significant in all cold environments or if this relationship is regionally-specific to Antarctica.

### 4.4. Downcore application of the global and new Antarctic and sub-Antarctic brGDGT–temperature calibrations

We applied both the global Pearson et al. (2011) and our new Antarctic and sub-Antarctic brGDGT–temperature calibration to a sediment core from Fan Lake, Annenkov Island, South Georgia to evaluate the use of both calibrations as a palaeothermometer (Fig. 5a and 5f). The GDGT–temperature records from Fan Lake were compared with pollen and total organic content (TOC) data from the lake alongside the Bentley et al. (2009) Antarctic Peninsula climate synthesis record (Fig. 5). The Fan Lake sediment core was dated to c. 7700 cal yr BP (see Strother et al., 2015). Here, we focused on the last 4000 years of the record as prior to c. 4300 cal yr BP the lake was influenced by glaciolacustrine and deglaciation-related sedimentary processes.

The Antarctic and sub-Antarctic GDGT–temperature reconstruction for Fan Lake (Fig. 5a) showed the warmest conditions between c. 3800 to 3300 cal yr BP with additional peaks in temperature at c. 2600 and 600 cal yr BP. The former was consistent with the mid-Holocene warm period when drier/warmer conditions prevailed on South Georgia between c. 3800 and 2800 cal yr BP seen in the Fan Lake pollen record (Fig. 5b and 5c) and other records from South Georgia (e.g., Van der Putten et al., 2009). Another peak in temperature at c. 600 cal yr BP (Fig. 5a) also correlates well with the Strother et al. (2015) Fan Lake pollen record (Fig. 5b and 5c) between c. 900 and 700 cal yr BP. Although Strother et al. (2015) made no reference to a warm period at c. 2600 cal yr BP, drier and possibly warmer conditions were noted at Cumberland Bay, to the northeast of South Georgia, by Clapperton et al. (1989) at c. 2600 cal yr BP. Finally, 'colder' conditions reconstructed in the Strother et al. (2015) pollen record between c. 2200 and 1650 cal yr BP are also represented within the GDGT record.

The peaks in temperature during known extreme warm events particularly the mid-Holocene warm period (Fig. 5h), are much more prominent when applying our new GDGT–temperature calibration (Fig. 5a). The amplitude of warming seen when applying our new calibration is greater than represented in previous ice core records (e.g., Mulvaney et al., 2012). However, this could be due to an acceleration and greater amplitude of temperature change in sub-Antarctic lakes as a result of changes in their size. Contemporary seasonal reductions have been noted on nearby Signy Island (Ellis-Evans, pers. comm.) where lake volume reduces during the summer months (December to February). Therefore, during a period of sustained warming, such as the mid-Holocene warm period, there could have been a significant reduction in lake level and volume causing a greater amplification in lake temperature. This

implies that the Antarctic and sub-Antarctic calibration is likely performing better than the global calibration in Fan Lake which reconstructed a more subtle warming related to these events. This further emphasises the importance of GDGT-IIIb in Antarctic environments not only in the surface dataset but also when applying our new Antarctic and sub-Antarctic GDGT–temperature calibration downcore.

A more detailed reconstruction and interpretation of the GDGT–derived temperatures from Fan Lake will follow in forthcoming papers.

## 5. Conclusions

We found that GDGTs were present in all 32 Antarctic, sub-Antarctic and Southern Chilean lakes and that brGDGTs were dominant in 31 of the lakes studied.

Statistical tests showed that summer temperature was the primary environmental control on the composition of brGDGTs in Antarctic lakes, and that the effect of MSAT was largely independent of other limnological variables. This finding is consistent with other work in lacustrine environments and highlights the value of brGDGTs as a temperature proxy in cold environments.

The relationship between GDGT-IIIb and temperature in Antarctica is of particular importance, being near absent in lakes with a temperature lower than 1 °C, and absent below −0.5 °C. In addition, GDGT-IIIb was not significantly correlated to any of the other environmental variables.

The incorporation of GDGT-IIIb into our brGDGT–temperature calibration, together with GDGT-Ib, GDGT-II, and GDGT-III resulted in improved accuracy and precision ($r^2 = 0.83$, RMSE = 1.45 °C, RMSEP-LOO = 1.68 °C, RMSEP-H = 1.65 °C, $n = 36$) when compared to the application of the Pearson et al. (2011) global calibration to our Antarctic dataset (Eq. (3)) based on the same three compounds ($r^2 = 0.67$, RMSE = 2.00 °C, RMSEP-LOO = 2.23 °C, RMSEP-H = 2.37 °C, $n = 36$). GDGT-IIIb may also be important in other cold environments, for example the Arctic or high altitudes, meaning our new Antarctic calibration may be applicable in these environments.

The application of our regional lacustrine Antarctic and sub-Antarctic brGDGT–temperature calibration to sediment cores will enable us to substantially improve our understanding of past temperature in the region. A pilot study of a 4000 year record from Fan Lake, South Georgia based on our Antarctic and sub-Antarctic brGDGT–temperature calibration correlated well with key warm phases identified in previous research. The forthcoming extension of this record and additional records will explore these correlations in more detail and enable us to improve and expand our knowledge of palaeoclimates in the Southern Hemisphere.

## Acknowledgements

This study is an output of the British Antarctic Survey (BAS) Natural Environment Research Council (NERC)-funded Science Program, and was funded by NERC Studentship NE/J500173/1 to LF (BAS and Newcastle University) with additional support from: the European Commission under the 7th Framework Programme through the Action – IMCONet (FP7 IRSES, action No. 319718). We thank the BAS and HMS Endurance, the Australian Antarctic Division (AAD), the Alfred Wegener Institute Helmholtz Centre for Polar and Marine Research (AWI) (Germany), the Instituto Antártico Argentino (IAA), the South African National Antarctica program (SANAP), the National Institute of Polar Research (NIPR) (Japan) and BELSPO/University of Ghent (Belgium) for providing funding and field support to sites on the Antarctic Peninsula and on the South Shetland Islands (DH, EV, SR), to the Larsemann Hills and East Antarctica (EV, DH), Campbell Island (KS; Grant No. PZ00P2_136835), King George Island (SR, EP, DH), Marion Island (EV, DH), Syowa Oasis (EV, DH) and in Southern Chile (SR). Thanks go to Helen Talbot and Frances Sidgwick for running samples on the LC-MS at Newcastle University. Melanie Leng is thanked for running TOC data, which formed part of carbon and nitrogen isotope analysis for the Fan Lake core at the NERC National Isotope Geosciences Laboratory, Keyworth, UK. Finally, we thank Jeff Salacup and one anonymous reviewer for suggesting improvements to the original manuscript. All data presented in this paper is the property of BAS and collaborating organisations and are available on request from the Polar Data Centre (polardatacentre@bas.ac.uk).

## Appendix A. Supplementary material

Supplementary material related to this article can be found online at http://dx.doi.org/10.1016/j.epsl.2015.11.018.

## References

Anderson, L., Abbott, M.B., Finney, B.P., 2001. Holocene climate inferred from oxygen isotope ratios in lake sediments, central Brooks Range, Alaska. Quat. Res. 55, 313–321. http://dx.doi.org/10.1006/qres.2001.2219.

Bentley, M.J., Hodgson, D.A., Smith, J.A., Cofaigh, C.Ó., Domack, E.W., Larter, R.D., Roberts, S.J., Brachfeld, S., Leventer, A., Hjort, C., Hillenbrand, C.D., Evans, J., 2009. Mechanisms of Holocene palaeoenvironmental change in the Antarctic Peninsula region. Holocene 19 (1), 51–69. http://dx.doi.org/10.1177/0959683608096603.

Blaga, C.I., Reichart, G.J., Heiri, O., Sinninghe Damsté, J.S., 2009. Tetraether membrane lipid distributions in water-column particulate matter and sediments: a study of 47 European lakes along a north–south transect. J. Paleolimnol. 41 (3), 523–540. http://dx.doi.org/10.1007/s10933-008-9242-2.

Borcard, D., Gillet, F., Legendre, P., 2011. Numerical Ecology with R. Springer, Dordrecht.

Borcard, D., Legendre, P., Drapeau, P., 1992. Partialling out the spatial component of ecological variation. Ecology 73, 1045–1055. http://dx.doi.org/10.2307/1940179.

Braun, M., Saurer, H., Goßmann, H., 2004. Climate, energy fluxes and ablation rates on the ice cap of King George Island. Pesqui. Antart. Bras. 4, 87–103.

Burman, P., Chow, E., Nolan, D., 1994. A cross-validatory method for dependent data. Biometrika 81, 351–358.

Clapperton, C.M., Sugden, D.E., Birnie, J., Wilson, M.J., 1989. Late-Glacial and Holocene glacier fluctuations and environmental-change on South Georgia, Southern-Ocean. Quat. Res. 31 (2), 210–228. http://dx.doi.org/10.1016/0033-5894(89)90006-9.

Dean, W.E., 1974. Determination of carbonate and organic-matter in calcareous sediments and sedimentary-rocks by loss on ignition – comparison with other methods. J. Sediment. Petrol. 44 (1), 242–248.

Dray, S., Legendre, P., Peres-Neto, P.R., 2006. Spatial modelling: a comprehensive framework for principal coordinate analysis of neighbour matrices (PCNM). Ecol. Model. 196, 483–493. http://dx.doi.org/10.1016/j.ecolmodel.2006.02.015.

Edinger, J., Dutterweiler, D., Geyer, J., 1968. The response of water temperatures to meteorological conditions. Water Resour. Res. 4 (5), 1137–1143. http://dx.doi.org/10.1029/WR004i005p01137.

Gliozzi, A., Paoli, G., De Rosa, M., Gambacorta, A., 1983. Effect of isoprenoid cyclization on the transition temperature of lipids in thermophilic archaebacteria. Biochim. Biophys. Acta 735, 234–242. http://dx.doi.org/10.1016/0005-2736(83)90298-5.

Günther, F., Thiele, A., Gleixner, G., Xu, B., Yao, T., Schouten, S., 2014. Distribution of bacterial and archaeal ether lipids in soils and surface sediments of Tibetan lakes: implications for GDGT-based proxies in saline high mountain lakes. Org. Geochem. 67, 19–30. http://dx.doi.org/10.1016/j.orggeochem.2013.11.014.

Hodgson, D.A., Verleyen, E., Sabbe, K., Squier, A.H., Keely, B.J., Leng, M.J., Saunders, K.M., Vyverman, W., 2005. Late Quaternary climate-driven environmental change in the Larsemann Hills, East Antarctica, multi-proxy evidence from a lake sediment core. Quat. Res. 64 (1), 83–99. http://dx.doi.org/10.1016/j.yqres.2005.04.002.

Hopmans, E.C., Weijers, J.W., Schefuß, E., Herfort, L., Sinninghe Damsté, J.S., Schouten, S., 2004. A novel proxy for terrestrial organic matter in sediments based on branched and isoprenoid tetraether lipids. Earth Planet. Sci. Lett. 224 (1–2), 107–116. http://dx.doi.org/10.1016/j.epsl.2004.05.012.

Juggins, S., 2014. rioja: analysis of Quaternary science data. R package version (0.9–3), http://cran.r-project.org/package=rioja.

Kim, J.-H., Crosta, X., Willmott, V., Renssen, H., Bonnin, J., Helmke, P., Schouten, S., Sinninghe Damsté, J.S., 2012. Holocene subsurface temperature variability in the eastern Antarctic continental margin. Geophys. Res. Lett. 39. http://dx.doi.org/10.1029/2012GL051157. (L06705).

Kim, J.-H., Van der Meer, J., Schouten, S., Helmke, P., Willmott, V., Sangiorgi, F., Koç, N., Hopmans, E.C., Sinninghe Damsté, J.S., 2010. New indices and calibrations

derived from the distribution of crenarchaeal isoprenoid tetraether lipids: implications for past sea surface temperature reconstructions. Geochim. Cosmochim. Acta 74 (16), 4639–4654. http://dx.doi.org/10.1016/j.gca.2010.05.027.

Livingstone, D., Dokulil, M., 2001. Eighty years of spatially coherent Austrian lake surface temperatures and their relationship to regional air temperature and the North Atlantic Oscillation. Limnol. Oceanogr. 46 (5), 1220–1227. http://dx.doi.org/10.4319/lo.2001.46.5.1220.

Loomis, S.E., Russell, J.M., Ladd, B., Street-Perrott, F.A., Sinninghe Damsté, J.S., 2012. Calibration and application of the branched GDGT temperature proxy on East African lake sediments. Earth Planet. Sci. Lett. 357–358, 277–288. http://dx.doi.org/10.1016/j.epsl.2012.09.031.

Lumley, T., 2009. Leaps: regression subset selection. R package version 2.9. http://cran.r-project.org/web/packages/leaps/index.html.

Magand, O., Frezzotti, M., Pourchet, M., Stenni, B., Genoni, L., Fily, M., 2004. Climate variability along latitudinal and longitudinal transects in East Antarctica. Ann. Glaciol. 39, 351–358. http://dx.doi.org/10.3189/172756404781813961.

Mulvaney, R., Abram, N.J., Hindmarsh, R.C.A., Arrowsmith, C., Fleet, L., Triest, J., Sime, L.C., Alemany, O., Foord, S., 2012. Recent Antarctic Peninsula warming relative to Holocene climate and ice-shelf history. Nature 489 (7414), 141–204. http://dx.doi.org/10.1038/nature11391.

Naeher, S., Peterse, F., Smittenberg, R.H., Niemann, H., Zigah, P.K., Schubert, C.J., 2014. Sources of glycerol dialkyl glycerol tetraethers (GDGTs) in catchment soils, water column and sediments of Lake Rotsee (Switzerland) – Implications for the application of GDGT-based proxies for lakes. Org. Geochem. 66, 164–173. http://dx.doi.org/10.1016/j.orggeochem.2013.10.017.

Oksanen, J., Blanchet, F.G., Kindt, R., Legendre, P., Minchin, P.R., O'Hara, R.B., Simpson, G.L., Solymos, P., Stevens, H.M.H., Wagner, H., 2014. Vegan: community ecology package. R package version 2.3-0. http://cran.r-project.org/web/packages/vegan/index.html.

Pearson, E.J., Juggins, S., Talbot, H.M., Weckstrom, J., Rosen, P., Ryves, D.B., Roberts, S.J., Schmidt, R., 2011. A lacustrine GDGT–temperature calibration from the Scandinavian Arctic to Antarctic: renewed potential for the application of GDGT–paleothermometry in lakes. Geochim. Cosmochim. Acta 75 (20), 6225–6238. http://dx.doi.org/10.1016/j.gca.2011.07.042.

Peterse, F., van der Meer, J., Schouten, S., Weijers, J.W.H., Fierer, N., Jackson, R.B., Kim, J.-H., Sinninghe Damsté, J.S., 2012. Revised calibration of the MBT–CBT paleotemperature proxy based on branched tetraether membrane lipids in surface soils. Geochim. Cosmochim. Acta 96, 215–229. http://dx.doi.org/10.1016/j.gca.2012.08.011.

Peterse, F., Vonk, J., Holmes, M., Giosan, L., Zimov, N., Eglinton, T.I., 2014. Branched glycerol dialkyl glycerol tetraethers in Arctic lake sediments: sources and implications for paleothermometry at high latitudes. J. Geophys. Res., Biogeosci. 119, 1738–1754. http://dx.doi.org/10.1002/2014JG002639.

Powers, L.A., Johnson, T.C., Werne, J.P., Castañeda, I.S., 2005. Large temperature variability in the southern African tropics since the Last Glacial Maximum. Geophys. Res. Lett. 32, L08706. http://dx.doi.org/10.1029/2004GL022014.

Powers, L.A., Werne, J.P., Johnson, T.C., Hopmans, E.C., Damsté, J.S.S., Schouten, S., 2004. Crenarchaeotal membrane lipids in lake sediments: a new paleotemperature proxy for continental paleoclimate reconstruction? Geology 32 (7), 613–616. http://dx.doi.org/10.1130/G20434.1.

R Core Team, 2014. R: a language and environment for statistical computing. R foundation for statistical computing, Vienna, Austria. http://www.R-project.org/.

Roberts, S.J., Hodgson, D.A., Bentley, M.J., Sanderson, D.C.W., Milne, G., Smith, J.A., Verleyen, E., Balbo, A., 2009. Holocene relative sea-level change and deglaciation on Alexander Island, Antarctic Peninsula, from elevated lake deltas. Geomorphology 112 (1–2), 122–134. http://dx.doi.org/10.1016/j.geomorph.2009.05.011.

Roberts, S.J., Hodgson, D.A., Bentley, M.J., Smith, J.A., Millar, I.L., Olive, V., Sugden, D.E., 2008. The Holocene history of George VI Ice Shelf, Antarctic Peninsula from clast-provenance analysis of epishelf lake sediments. Palaeogeogr. Palaeoclimatol. Palaeoecol. 259 (2–3), 258–283. http://dx.doi.org/10.1016/j.palaeo.2007.10.010.

Rolland, N., Larocque, I., Francus, P., Pienitz, R., Laperriere, L., 2009. Evidence for a warmer period during the 12th and 13th centuries AD from chironomid assemblages in Southampton Island, Nunavut, Canada. Quat. Res. 72, 27–37. http://dx.doi.org/10.1016/j.yqres.2009.03.001.

Schoon, P.L., de Kluijver, A., Middelburg, J.J., Downing, J.A., Sinninghe Damsté, J.S., Schouten, S., 2013. Influence of lake water pH and alkalinity on the distribution of core and intact polar branched glycerol dialkyl glycerol tetraethers (GDGTs) in lakes. Org. Geochem. 60, 72–82. http://dx.doi.org/10.1016/j.orggeochem.2013.04.015.

Schouten, S., Hopmans, E.C., Schefuß, E., Sinninghe Damsté, J.S., 2002. Distributional variations in marine crenarchaeotal membrane lipids: a new tool for reconstructing ancient sea water temperatures? Earth Planet. Sci. Lett. 204, 265–274. http://dx.doi.org/10.1016/S0012-821X(02)00979-2.

Shanahan, T.M., Hughen, K.A., Van Mooy, B.A.S., 2013. Temperature sensitivity of branched and isoprenoid GDGTs in Arctic lakes. Org. Geochem. 64, 119–128. http://dx.doi.org/10.1016/j.orggeochem.2013.09.010.

Sinninghe Damsté, J.S., Ossebaar, J., Abbas, B., Schouten, S., Verschuren, D., 2009. Fluxes and distribution of tetraether lipids in an equatorial African lake: constraints on the application of the $TEX_{86}$ palaeothermometer and BIT index in lacustrine settings. Geochim. Cosmochim. Acta 73 (14), 4232–4249. http://dx.doi.org/10.1016/j.gca.2009.04.022.

Sinninghe Damsté, J.S., Ossebaar, J., Schouten, S., Verschuren, D., 2012. Distribution of tetraether lipids in the 25-ka sedimentary record of Lake Challa: extracting reliable $TEX_{86}$ and MBT/CBT palaeotemperatures from an equatorial African lake. Quat. Sci. Rev. 50, 43–54. http://dx.doi.org/10.1016/j.quascirev.2012.07.001.

Smith, J.A., Bentley, M.J., Hodgson, D.A., Roberts, S.J., Leng, M.J., Lloyd, J.M., Barrett, M.S., Bryant, C., Sugden, D.E., 2007. Oceanic and atmospheric forcing of early Holocene ice shelf retreat, George VI Ice Shelf, Antarctica Peninsula. Quat. Sci. Rev. 26 (3–4), 500–516. http://dx.doi.org/10.1016/j.quascirev.2006.05.006.

Street-Perrott, F.A., Barker, P.A., Swain, D.L., Ficken, K.J., Wooller, M.J., Olago, D.O., Huang, Y., 2007. Late Quaternary changes in ecosystems and carbon cycling on Mt. Kenya, East Africa: a landscape-ecological perspective based on multi-proxy lake-sediment influxes. Quat. Sci. Rev. 26 (13–14), 1838–1860. http://dx.doi.org/10.1016/j.quascirev.2007.02.014.

Strother, S.L., Salzmann, U., Roberts, S.J., Hodgson, D.A., Woodward, J., Van Nieuwenhuyze, W., Verleyen, E., Vyverman, W., Moreton, S.G., 2015. Holocene vegetation and change of westerly winds reconstructed from a high-resolution sub-Antarctic pollen record at Fan Lake, South Georgia. Holocene 25 (2), 263–279. http://dx.doi.org/10.1177/0959683614557576.

Sun, Q., Chu, G., Liu, M., Xie, M., Li, S., Ling, Y., Wang, X., Shi, L., Jia, G., Lü, H., 2011. Distributions and temperature dependence of branched glycerol dialkyl glycerol tetraethers in recent lacustrine sediments from China and Nepal. J. Geophys. Res. 116. http://dx.doi.org/10.1029/2010JG001365. (G01008).

Telford, R.J., Birks, H.J.B., 2005. The secret assumption of transfer functions: problems with spatial autocorrelation in evaluating model performance. Quat. Sci. Rev. 24 (20–21), 2173–2179. http://dx.doi.org/10.1016/j.quascirev.2005.05.001.

Tierney, J.E., Russell, J.M., Eggermont, H., Hopmans, E.C., Verschuren, D., Sinninghe Damsté, J.S., 2010. Environmental controls on branched tetraether lipid distributions in tropical East African lake sediments. Geochim. Cosmochim. Acta 74 (17), 4902–4918. http://dx.doi.org/10.1016/j.gca.2010.06.002.

Tierney, J.E., Russell, J.M., Huang, Y., Sinninghe Damsté, J.S., Hopmans, E.C., Cohen, A., 2008. Northern hemisphere controls on tropical southeast African climate during the past 60,000 years. Science 322 (5899), 252–255. http://dx.doi.org/10.1126/science.1160485.

Tierney, J.E., Tingley, M.P., 2014. A Bayesian, spatially-varying calibration model for the $TEX_{86}$ proxy. Geochim. Cosmochim. Acta 127, 83–106. http://dx.doi.org/10.1016/j.gca.2013.11.026.

Uda, I., Sugai, A., Itoh, Y.H., Itoh, T., 2001. Variation in molecular species of polar lipids from thermoplasma acidophilum depends on growth temperature. Lipids 36 (1), 103–105. http://dx.doi.org/10.1007/s11745-001-0914-2.

Van der Putten, N., Verbruggen, C., Ochyra, R., Spassov, S., de Beaulieu, J.-L., De Dapper, M., Hus, J., Thouveny, N., 2009. Peat bank growth, Holocene palaeoecology and climate history of South Georgia (sub-Antarctica), based on a botanical macrofossil record. Quat. Sci. Rev. 28 (1–2), 65–79. http://dx.doi.org/10.1016/j.quascirev.2008.09.023.

Verleyen, E., Hodgson, D.A., Vyverman, W., Roberts, D., McMinn, A., Vanhoutte, K., Sabbe, K., 2003. Modelling diatom responses to climate induced fluctuations in the moisture balance in continental Antarctic lakes. J. Paleolimnol. 30 (2), 195–215. http://dx.doi.org/10.1023/A:1025570904093.

Watcham, E.P., Bentley, M.J., Hodgson, D.A., Roberts, S.J., Fretwell, P.T., Lloyd, J.M., Larter, R.D., Whitehouse, P.L., Leng, M.J., Monien, P., Moreton, S.G., 2011. A new Holocene relative sea level curve for the South Shetland Islands, Antarctica. Quat. Sci. Rev. 30 (21–22), 3152–3170. http://dx.doi.org/10.1016/j.quascirev.2011.07.021.

Webb, B., Nobilis, F., 1997. Long-term Perspective on the nature of the air–water temperature relationship: a case study. Hydrol. Process. 11, 137–147. http://dx.doi.org/10.1002/(SICI)1099-1085(199702)11:2<137::AID-HYP405>3.0.CO;2-2.

Weijers, J.W.H., Schefuß, E., Schouten, S., Sinninghe Damsté, J.S., 2007b. Coupled thermal and hydrological evolution of tropical Africa over the last deglaciation. Science 315 (5819), 1701–1704. http://dx.doi.org/10.1126/science.1138131.

Weijers, J.W.H., Schouten, S., Spaargaren, O.C., Sinninghe Damsté, J.S., 2006. Occurrence and distribution of tetraether membrane lipids in soils: implications for the use of the $TEX_{86}$ proxy and the BIT index. Org. Geochem. 37 (12), 1680–1693. http://dx.doi.org/10.1016/j.orggeochem.2006.07.018.

Weijers, J.W.H., Schouten, S., Van den Donker, J.C., Hopmans, E.C., Sinninghe Damsté, J.S., 2007a. Environmental controls on bacterial tetraether membrane lipid distribution in soils. Geochim. Cosmochim. Acta 71 (3), 703–713. http://dx.doi.org/10.1016/j.gca.2006.10.003.

Woltering, M., Atahan, P., Grice, K., Heijnis, H., Taffs, K., Dodson, J., 2014. Glacial and Holocene terrestrial temperature variability in subtropical east Australia as inferred from branched GDGT distributions in a sediment core from Lake McKenzie. Quat. Res. 82 (1), 132–145. http://dx.doi.org/10.1016/j.yqres.2014.02.005.